50. SYNTHESIS OF PHYSICAL PROPERTIES DATA FROM DSDP LEG 41

P.K. Trabant, Texas A&M University, College Station, Texas

INTRODUCTION

Physical properties measured during Leg 41 include mass bulk physical properties (wet and dry density, water content, void ratio, and porosity), sound velocities, shear strengths, drilling rates, and a limited number of laboratory consolidation tests. As stated by Rocker (1974a) the term "physical properties" consists strictly of laboratory or shipboard "measurements" performed upon "least disturbed" samples, and do not necessarily reflect true in situ values. Certain variations of measured properties with respect to in situ conditions are discussed.

Variations in standard shipboard procedures employed during Leg 41 are described and followed by a tabulation of the measured physical properties. A discussion follows of the interrelationship between the physical properties and sedimentological data for each of the five investigated sites.

TEST PROCEDURES EMPLOYED DURING LEG 41

Shear Strength

Shear strengths were measured on recovered samples by means of a miniature vane shear device as employed by Bennett and Keller (1973), Lee (1973), and Rocker (1974b) during DSDP Legs 16, 19, and 29, respectively. A thorough discussion of the miniature vane apparatus has been presented by Boyce (1973a).

The miniature vane employed measured approximately 0.5 × 0.5 in. (height × diameter). Torque was applied through a calibrated spring at a rotation rate of about 90° per min. A simple nomogram employing the spring calibration results was constructed to facilitate rapid conversion from angle of rotation to shear strength. It is to be noted that the term "shear strength" as measured by the miniature vane apparatus refers to the "cohesion" of the clays and silts measured in an undrained, unconsolidated condition. Few shear strength measurements were performed during Leg 41, due to the small number of retrieved samples within the uppermost soft sediments at most sites, in order to reach important site objectives.

Mass Bulk Properties Measurements

The following mass bulk sediment properties were measured onboard: bulk density or wet unit weight, water content, void ratio, porosity, and specific gravity of solids. A number of GRAPE (Gamma Ray Attenuation Porosity Evaluator) values were determined for small subsamples tested for physical properties measurements, and are tabulated and discussed later in conjunction with each site. A description of the GRAPE method and results has been presented by Boyce (1975).

During Leg 41 several of the standard mass bulk property measurement techniques (syringe, displaced water, and full section weight methods) were discarded and the following technique employed; wet volume and mass determinations were made on 10-15 g samples by means of an air-comparison pycnometer, employing helium gas for purging, and a triple beam balance. Samples were subsequently dried at 105°C for 18-24 hr. Then the dry volume and weight of the samples were determined and the mass bulk physical properties computed by:

(1) Bulk density $= \dfrac{\text{wet weight (gm/cc)}}{\text{wet volume}}$

(2) Water content (% dry weight) $= \dfrac{\text{weight water \%}}{\text{weight solids}}$

(3) Porosity $= \dfrac{\text{volume of water \%}}{\text{volume solids + water}}$

(4) Void ratio $= \dfrac{\text{volume water,}}{\text{volume solids}}$ assuming saturation

(5) Specific gravity of solids $= \dfrac{\text{weight solids}}{\text{volume solids}}$ assuming water density of 1.0 g/cc

The above method is a common geotechnical laboratory technique and has frequently been employed for postcruise analyses (i.e., Keller and Bennett, 1973, Rocker, 1974a). The method produces accuracies on the order of a few percent with proper calibration of the pycnometer and balance, and proved both satisfactory and simple as a routine shipboard procedure during Leg 41.

Sound Velocity Measurements

The Hamilton frame apparatus was used to measure compressional wave velocities at a frequency of 400 kHz. The technique, theory, and calibration method have been presented by Boyce (1973b, 1975).

A slight modification of the procedure described by Boyce (1973b) was employed during Leg 41, whereby both the start and stop times of the accoustic pulses were measured through several media and a regression analysis performed to determine the delay time factor $\triangle$T (intercept) as illustrated in Figure 1. This method also permitted measurement of velocities for the calibration standards (slope of X versus t plot, Figure 1).

Thus, velocities were obtained by measuring sample thickness D, start time T_1, and arrival time T_2. Velocities were then computed by:

$$V_p = \frac{(T_2 - T_1) - \triangle T}{D} \text{ in } \mu\text{sec/cm}$$

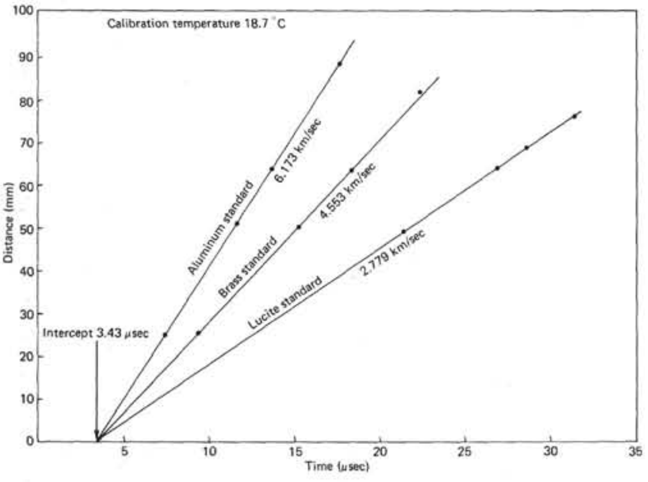

Figure 1. *Velocimeter calibration curves.*

Difficulties were encountered when measuring velocities of soft sediments which had to be made through split liners, the results exhibited inconsistencies due to inaccuracies in the determination of sample thickness and the presence of drilling slurry between sample and liner. The velocity measurements were performed in both the vertical and horizontal directions where feasible, in order to determine acoustic anisotropy.

Consolidation Tests

Laboratory consolidation tests, with applied back pressure, were performed upon several samples obtained during Leg 41 for the purpose of determining preconsolidation pressures. A discussion of the procedures and purposes of these tests has been presented by Trabant et al. (1975) and Hottman (in press) for samples obtained on DSDP Legs 31 and 40. The results are discussed herein along with the accompanying e-logp curves and overburden calculations.

SUMMARY OF SHEAR STRENGTH MEASUREMENTS

Only a few cores were retrieved within the uppermost soft sediments at Sites 366 and 367, the results of which are listed in Table 1. Strength measurements are plotted versus depth for Sites 368 through 370 in Figure 2.

Site 368

Shear strength measurements at this site display a slight increase in value to a depth of 233 meters, where the volcanic shard zone is encountered. A value of 1.05 kg/cm² is associated with the shard zone while the underlying stiff clays soon exceed the maximum measurable value of 5.0 kg/cm² below a depth of 289 meters. The latter increase corresponds approximately to the top of Lithologic Unit 2A, where a facies change from calcareous oozes and marls to clays and claystone occurs.

Site 369

Shear strength data gathered at this site reveal a "geotechnic break" or marked increase in strength values at a depth of 40 meters as illustrated in Figure 2. Although there appears to be no observed lithologic change, shear strength values suddenly increase from less than 1.0 kg/cm² to well over 3.0 kg/cm². This abrupt increase in strength values corresponds to the Pliocene/Miocene boundary and suggests the possible removal perhaps by slumping of sediments from above the boundary prior to the onset of Pliocene sedimentation. It is also possible that an undetected change in geochemical or sedimentological properties is the cause for this unusual increase in shear strength. Below a depth of 180 meters shear strengths are above 5 kg/cm², the maximum values measurable with the minature vane apparatus.

Site 370

Shear strength data were obtained at this site within each of the first five cores retrieved to a depth of 326 meters. Miniature vane values obtained on chunks of undisturbed material were employed as the widely spaced coring program produced heavily disturbed samples. The sparsity of data reveals unusually low shear strengths at a depth of 208 meters, indicating a relatively under consolidated material. Maximum shear strengths above 5 kg/cm² are encountered at 325 meters which is slightly deeper than the previous four sites. It thus appears that the upper 300 meters at Site 370 may be slightly under consolidated relative to previously drilled sites during Leg 41.

MASS BULK PROPERTIES AND VELOCITIES

Porosity values and acoustic velocities measured onboard during Leg 41 are shown in Figures 3 through 7 to illustrate the variation of sediment mass properties with depth. Additional mass property data are listed in Table 1.

Site 366 (Hole 366A)

This site was located on the Sierra Leone Rise and drilled to a total depth of 850 meters. Sediments consisted of nanno oozes and marls grading into chalks limestones and marlstones with occasional interbedded cherts and porcellanites. The porosities depicted in Figure 3 show a moderate decrease from 70% within the uppermost nanno oozes to about 50% at the base of Lithologic Unit 2 at a depth of 480 meters. Porosities thus decrease approximately 20% within the nanno oozes, marls, and chalks of the first 460 meters. This reduction in void space is essentially attributable to the effects of compaction caused by the increase in overburden pressure associated with these depths.

Similarly the velocity data illustrated in Figure 3 show a slight increase from 1.5 km/sec at the sea floor to approximately 2.0 km/sec at the base of Lithologic Unit 2. Within the underlying Lithologic Units 3 and 4, however, there is a rapid reduction in porosity to values approaching 10%. This marked reduction in void space is associated with the lithification of pelagic sediments comprising Lithologic Units 3 and 4, which are composed of siliceous and argillaceous limestones with interbedded cherts and porcellanites. Velocities measured within these units attain values close to 4.0 km/sec within the cherts and porcellanites, while the

TABLE 1
Physical Properties Measurements for Leg 41

Core-Section	Sample Depth (m)	GRAPE Density (g/cc)	GRAPE Porosity (%)	Pycnometer Density (g/cc)	Pycnometer Porosity (%)	Pycnometer Water Content (%)	Velocity (km/sec) Vertical	Velocity (km/sec) Horizontal	Shear Strength (kg/cm^2)	Minutes Drilling Rate	Visual Description
Site 366											
4-2	245	1.711	58	1.906	57	57				9	Nanno ooze
5-5	374			2.000	51	41				15	Nanno chalk
6-3	379			2.007	51	43				15	Nanno chalk
7-2	389			1.947	48	36		1.892		15	Nanno chalk
8-2	397			1.765	55	47	1.845	1.772		12	Nanno chalk
9-3	408			2.102	42	29	1.895	1.877		25	Nanno chalk
10-2	416			1.904	50	37	1.743	1.692		21	Nanno chalk
11-1	423			1.807	53	46	1.699	1.692		35	Nanno chalk
12-3	436			1.933	46	32	1.850	1.857		24	Nanno chalk
13-2	444			1.858	52	39				33	Nanno chalk
14-3	455			1.668	59	55	1.850	1.857		20	Nanno chalk
15-1	462			2.059	39	25	2.178	1.921		27	Nanno chalk
16-2	472			2.043	39	25	1.943	1.939		35	Nanno chalk
17-2	480			2.181	37	24	2.094	2.082		60	Nanno chalk
18-1	490			2.116	37	20				50	Nanno chalk
19-1	499						2.161	2.089		45	Nanno chalk
20-2	511							2.029		75	Nanno chalk
21-2	520			2.313	28	13		2.391		75	Nanno chalk
22-1	528			2.381	62	7	3.594	3.761		55	Chert/porcellanite
22-1	528			2.606	15	13	2.463	2.525			Silicified limestone
23-1	538			2.332	11	6	4.075	4.129		75	Chert/porcellanite
23-1	538			2.393	19	8	2.743	2.837			Silicified limestone
24-2	548			2.318	14	7	3.512	3.849		110	Chert/porcellanite
24-2	549			2.474	18	9	2.805	2.875			Silicified limestone
25-2	558			2.293	14	8				73	Silicified limestone
26-3	569			2.264	28	13				73	Silicified limestone
27-2	577			2.219	27	13				68	Silicified limestone
28-3	588			2.263	27	13	2.519	2.521		72	Silicified limestone
29-2	596			2.319	24	12	2.451	2.582		47	Argillaceous limestone
30-1	605			2.310	9	6		3.706		75	Chert
31-2	615			1.914	46	31		2.234		72	Argillaceous limestone
36-3	664			1.915	45	27		1.977		35	Argillaceous limestone
37-3	673			1.997	44	29		1.943		35	Argillaceous limestone
38-3	683			1.967	41	25	2.155	2.238		28	Argillaceous limestone
39-3	693			2.094	37	21	2.188	2.293		29	Argillaceous limestone
40-3	702			2.031	38	22	2.150	2.183		38	Argillaceous limestone
41-3	712			2.130	35	20	2.597	2.670		29	Argillaceous limestone
42-3	722			2.298	26	13	2.389	2.897		46	Argillaceous limestone
43-3	732			2.298	26	12	2.675	2.701		48	Siliceous limestone
44-3	740			2.081	41	26	1.951	2.118		82	Calcarenite
45-3	749			2.396	23	11	2.661	2.858		90	Siliceous limestone
46-3	759			2.386	25	13	2.547	2.749		90	Siliceous limestone
47-3	769			2.394	22	11	2.443	2.640		100	Siliceous limestone
48-3	778			2.371	24	12	2.445	2.502		95	Siliceous limestone
49-3	789						2.502	2.769		48	Siliceous limestone
50-3	798			2.392	24	12	2.505	2.842		71	Siliceous limestone
Hole 366A											
2-3	10	1.538	68	1.595	70	92		1.654		3	Nanno marl
5-3	38	1.626	63	1.615	67	78		1.533		3	Nanno marl
6-3	48	1.643	62	1.558	68	80		1.547		3	Nanno marl
7-3	57			1.673	64	64		1.523		2	Nanno marl
9-3	76	1.651	61	1.632	64	67		1.513		2	Nanno ooze
12-3	105	1.755	55	2.036	51	55		1.528		6	Nanno ooze
14-3	124	1.774	54	1.732	60	56		1.557		8	Nanno ooze
15-3	134	1.739	56	1.785	57	49		1.587		8	Nanno ooze
16-3	143	1.749	55	1.743	58	51		1.493		14	Clay/marl/ooze breccia
17-3	156	1.699	59					1.584		12	Clay/marl/ooze breccia
18-3	162			1.678	61	57				11	Nanno marl/chalk
20-3	181	1.692	59	1.671	62	59				18	Nanno chalk
21-3	191	1.698	59	1.705	60	56		1.671		16	Nanno chalk
23-3	210			1.475	73	105				7	Nanno chalk
24-2	217			1.635	64	66				4	Nanno chalk
26-3	238			1.677	62	60				6	Nanno chalk
27-3	248			1.741	59	51				8	Clay and nanno chalk
28-3	257			1.726	58	52				6	Clay and nanno chalk
29-3	266			1.806	54	44		1.671		8	Clay and nanno chalk
30-3	276			1.824	51	40				10	Clay and nanno chalk
31-3	285			1.794	54	44				10	Clay and nanno chalk
33-3	304			1.891	51	40		1.685		8	Clay and nanno chalk
34-3	314			1.883	50	39		1.803		8	Clay and nanno chalk
35-3	323			1.967	47	36		1.699		8	Clay and nanno chalk

TABLE 1 – *Continued*

Core-Section	Sample Depth (m)	GRAPE Density (g/cc)	GRAPE Porosity (%)	Pycnometer Density (g/cc)	Pycnometer Porosity (%)	Pycnometer Water Content (%)	Velocity (km/sec) Vertical	Velocity (km/sec) Horizontal	Shear Strength (kg/cm²)	Minutes Drilling Rate	Visual Description
Site 366A											
36-3	333			1.951	47	35		1.833		8	Clay and nanno chalk
37-3	342			1.912	49	36		1.725		11	Clay and nanno chalk
38-3	351			1.897	49	37		1.718		9	Clay and nanno chalk
Site 367											
4-2	66	1.668	60	1.645	65	66				7	Marl and sand
4-3	68	1.760	55	1.656	62	63		1.489			Marl and sand
6-1	237	1.689	59	1.900	50	41		1.573	0.43	22	Marl and silty clay
8-3	306			1.515	64	74		1.645		13	Clay
8-3	306			1.369	74	115		1.663	too stiff		Clay
13-3	373			1.860	39	29			too stiff	79	Zeolitic clay and sand
13-3	373	1.553	68	1.706	65	60			too stiff		Zeolitic clay
14-3	383			1.656	69	68				58	Zeolitic clay and sand
15-3	477			1.953	49	34				36	Silty clay and sand
15-4	479			1.933	50	35					Silty clay and sand
16-3	544			1.939	48	33				34	Silty clay
17-3	620			1.502	54	55				44	Clay
18-3	640			1.412	40	42				53	Black shale
19-4	650			1.856	47	32				65	Black shale
19-4	650			1.560	42	37					Black shale
20-4	695			1.667	46	38				43	Black shale
21-3	695			1.703	45	36				24	Black shale
21-6	700			1.847	44	29	1.595				Black shale
21, CC	701			2.665	8	3	3.680	4.016			Limestone
22-3	724			1.951	45	30				53	Shale/clay/silt
24-2	837			1.093	41	25				38	Claystone
24-2	837			2.129	37	21				38	Claystone
24-3	838			2.087	45	26					Claystone
25-3	895			2.405	20	8	3.308	3.438		80	Limestone
26-3	914			2.298	27	12				60	Limestone/marlstone
27-3	943			2.342	23	12	3.137	3.007		50	Limestone/marlstone/shale
27-3	943			2.171	27	9	2.510	3.500			Limestone/marlstone/shale
29-2	998			2.632	9	4	4.435	4.271		40	Limestone
29-2	999			2.462	17	7	2.862	3.167			Marlstone
30-1	1026			2.296	28	15	1.928	2.330		70	Argillaceous limestone
31-2	1055			2.520	15	6	3.778	3.647		60	Limestone
32-3	1086			2.426	18	8	3.934	4.220		75	Limestone/porcellanite
33-1	1106			2.458	16	7	3.435	3.681		127	Limestone
33-2	1107			2.693	6	2	3.205	3.779			Limestone
33-3	1109			2.481	17	7					Argillaceous limestone
35-3	1123			2.487	15	7	3.076	3.513		274	Limestone
35-3	1123			2.567	10	4	4.198	4.183			Limestone
36-3	1131			2.425	21	10	2.501	2.931		135	Argillaceous limestone
39-2	1150							4.260		240	Basalt
Site 368											
1-3	4	1.544	68	1.468	73	104			0.45	2	Marl
2-3	13	1.570	66	1.553	70	86			0.55	3	Marl
3-3	51	1.569	67	1.522	71	74			0.15	8	Marl and ooze
4-3	89	1.653	61	1.590	67	76		1.497	0.42	20	Marl and ooze
5-3	127	1.647	62	1.624	66	71		1.518	0.12	21	Nanno ooze
6-3	165	1.842	50	1.704	60	56		1.487	0.16	18	Nanno ooze
7-3	174	1.788	53	1.661	64	64		1.506	0.22	19	Nanno ooze and marl
7-3	175			1.856	53	40		1.483			Nanno ooze and marl
8-5	187	1.889	49	1.946	64	95				19	Nanno marl
9-1	193			1.873	52	38				11	Nanno marl and clay
10-2	201			1.809	56	45		1.640	0.82	20	Clay
11-3	212			1.812	55	45		1.526	1.65	16	Silty clay
13-4	233	1.583	66	1.622	67	74		1.516	1.05		Volcanic shards
13-4	233			1.621	60	23		1.445	1.05	23	Volcanic shards
14-3	241	1.628	63	1.586	68	78		1.544	5.0	22	Stiff clay
15-3	250	1.482	73	1.444	76	115				31	Silty clay
17-3	269	1.814	51	1.848	53	40		1.584	4.5		Silty clay
17-6	274	1.814	51	1.878	52	37				67	Silty clay
18-3	279	1.846	50	1.852	53	39			5.0	85	Silty clay
19-3	289	1.785	53	1.733	71	54				51	Silty clay
21-2	315	1.505	70	1.579	69	78					
22-3	327	1.537	69	1.549	52	80		1.758		32	Gassy claystone
22-5	330			1.518	71	84		1.514			Gassy claystone
25-1	371			1.961	26	21		3.286		66	Porcellanite
25-1	370			1.484	74	97					Claystone
27-1	386			1.791	48	34	2.833	2.859		44	
28-1	395			1.636	59	61				39	Clay/silt stone
31-3	431	1.534	69	1.660	61	62				68	Clay/silt stone
32-3	440	1.495	71	1.659	64	63				63	Clay/silt stone

TABLE 1 – *Continued*

Core-Section	Sample Depth (m)	Density (g/cc)	Porosity (%)	Pycnometer Density (g/cc)	Pycnometer Porosity (%)	Pycnometer Water Content (%)	Velocity (km/sec) Vertical	Velocity (km/sec) Horizontal	Shear Strength (kg/cm^2)	Minutes Drilling Rate	Visual Description
Site 368											
34-2	468			1.555	66	75				75	Clay stone
36-3	516			1.564	68	72				72	Clay stone
37-5	537			1.653	67	54	1.427			57	Clay stone
38-3	564			1.676	63	56				100	Clay stone
39-3	573			1.713	58	51		1.637		90	Clay stone
40-4	585			2.818	7	3		5.009		60	Porcellanite
41-3	593			1.656	57	60				72	Clay stone/siltstone
42-3	593			1.720	58	52				55	Clay stone/siltstone
42-3	601			1.827	47	40		1.631		80	Clay stone/siltstone
43-4	613			1.647	62	57					Clay stone/siltstone
44-3	621			1.644	57	56				110	Clay stone/siltstone
45-3	630			1.767	60	46		1.745		108	Clay stone/siltstone
46-3	641			1.916	52	37	1.602	1.469		43	Clay stone/siltstone
47-3	650			1.905	49	34				36	Clay stone/siltstone
50-3	706			2.042	46	26				26	Silty shale
51-3	715			2.073	42	25				45	Shale
52-4	727			2.027	43	28				43	Silty shale
52-4	727			2.010	48	31					Silty shale
53-3	754			2.032	44	25	1.767			48	Silty clay stone
54-4	803			2.063	42	24				49	Silty clay stone
55-3	841			2.059	40	26	2.124			72	Silty clay stone
57-4	898			2.023	45	32				47	Shale
58-3	924			2.064	41	24				39	Shale
59-3	942			2.197	53	66				87	Sand shale
60-2	951			2.567	17	8	3.550			82	Diabase
60-4	954			2.145	32	17		3.055			Shale/clay stone
63-3	979			1.847	35	23				150	Shale/clay stone
Hole 369											
1-3	3	1.851	51	1.801	57	46			0.48	2	Nanno ooze
2-3	8	1.829	51	1.803	56	47		1.67	0.58	20	Nanno ooze
3-3	18			1.762	58	50		1.65	0.52	19	Nanno ooze
4-3	27			1.803	56	47		1.59	0.27	31	Nanno marl
5-4	38			1.823	55	44		1.60	0.70	13	Nanno marl
Hole 369A											
1-3	46			1.793	57	46			3.25	11	Clayey nanno marl
2-3	55			1.794	55	47		1.63	4.00	7	Clayey nanno marl
3-3	65			1.850	54	43				7	Nanno marl
4-3	75			1.832	56	50		1.62	3.60	8	Nanno marl
5-3	84			1.898	52	42		1.66		8	Nanno marl
5-6	89			1.639	64	68	1.74	1.70		8	Nanno marl
6-3	94			1.945	46	36					Nanno marl
6-6	98			1.849	53	41		1.68			Nanno marl
7-3	103			1.867	54	25		1.67	3.50	15	Nanno marl
8-3	113			1.859	55	43		1.67		19	Nanno marl
9-1	119			1.824	57	48	1.575	1.602		14	Nanno marl
9-3	122			1.824	53	43		1.73			Nanno marl
10-3	131			1.845	52	41		1.66	4.50	18	Nanno marl
11-3	141			1.640	61	61		1.65	5.00+	11	Nanno marl
12-3	151			1.495	68	88		1.61	5.00	8	Nanno marl
14-3	169			1.711	56	51			5.00	11	Nanno marl
15-3	179			1.862	47	36			5.00	11	Nanno marl
17-2	198			1.786	57	46		1.75		22	Nanno marl
18-3	207			1.750	57	48				20	Nanno marl
19-3	217			1.775	55	46		1.73		13	Nanno marl
20-3	227			1.855	51	38		1.78		11	Nanno marl
21-3	235			1.825	55	42		1.78		12	Nanno marl
22-3	245			1.899	49	36		1.78		13	Nanno marl
23-3	255			1.831	53	40		1.78		10	Nanno marl
24-3	264			1.978	44	32				13	Nanno marl
25-3	274			1.783	55	45				12	Nanno marl
26-3	283			2.016	43	28				18	Nanno Marl
27-3	293			1.846	52	39		1.83		20	Nanno marl
28-3	302			1.847	53	40		1.84		16	Nanno marl
29-3	311			1.923	48	34		1.75		14	Nanno marl
32-1	337			1.817	54	42		1.88		27	Nanno marl
33-3	350			1.776	50	40		1.85			Nanno marl
34-2	352			1.957	46	32	1.934	1.912		24	Nanno marl
34-2	358			2.157	14	11	3.839	3.937		20	Porcellanite
35-1	366			1.966	46	29	1.832	1.868		36	Argillaceous limestone
36-3	378			2.134	37	23	1.947	1.952		22	Argillaceous limestone
37-3	388			1.979	43	27	1.990	2.078		35	Nanno marlstone
38-2	396			1.952	40	28				36	Nanno marlstone

TABLE 1 – *Continued*

Core-Section	Sample Depth (m)	GRAPE Density (g/cc)	GRAPE Porosity (%)	Pycnometer Density (g/cc)	Pycnometer Porosity (%)	Pycnometer Water Content (%)	Velocity (km/sec) Vertical	Velocity (km/sec) Horizontal	Shear Strength (kg/cm²)	Minutes Drilling Rate	Visual Description
Site 369A											
38-3	398			2.168	37	24	1.843	1.972			Nanno marlstone
39-3	406			2.175	34	19				50	Argillaceous chalk
40-4	418			2.052	41	27				31	Argillaceous chalk
41-2	424			2.104	38	22	1.891	2.052		38	Nanno marl/slump
42-3	435			1.937	49	36		1.556		63	Argillaceous chalk
43-4	447			2.465	18	7	2.986	3.323		73	Nanno marlstone
44-2	453			2.540	14	6		3.337		62	Silty nanno chalk
45-3	463			1.985	45	30	1.595			59	Nanno marl/chalk
46-3	473			2.669	6	3	3.215	3.718		78	Marl and gypsum
47-3	483			2.033	39	36				83	Silty nanno marl/chalk
Site 370											
1-3	4			1.918	52	41			0.65	2	Silty clay
2-2	105			1.987	51	36		1.598	1.64	11	Silty clay
3-1	208			1.907	51	40		1.545	0.72	12	Silty clay
3-1	208			1.800	55	45		1.603	0.62		Silty clay
4-3	220			1.929	47	36		1.652		12	Silty clay
5-3	325			1.907	52	38		1.662	3.7		Silty clay
5-3	325			2.042	43	27		1.786	5.0	34	Silty clay
6-2	428			2.094	37	24	2.054	1.993		55	Silty clay
8-2	466			2.154	32	18	2.139	2.419		57	Silty clay
9-1	483			1.915	45	29	2.019	2.189		60	Silty clay
9, CC	485			2.113	11	12		2.788			Porcellanite
10-2	504			2.114	34	10	2.426	2.688		81	Claystone
13-2	551			2.176	26	15		3.258		43	Porcellanite
13-2	552			1.929	56	27		2.141			Claystone
13-2	552			2.610	10	4		3.699			Porcellanite
14-1	569			1.932	47	33	2.308	1.920		45	Calcareous siltstone
15-3	592			2.042	40	27	1.850	2.227		33	Calcareous siltstone
16-2	608			2.054	48	28				61	Calcareous claystone
16-3	610			1.886	48	61					Calcareous claystone
17-2	618			2.131	35	22	1.871	2.258		81	Calcareous claystone
19-1	655			2.190	36	20	1.849	2.035		49	Calcareous claystone
20-2	676			2.594	9	3	4.301	4.369		112	Argillaceous limestone
21-2	684			2.098	39	24				60	Claystone
22-3	695			2.284	40	27				68	Shale
23-3	705			2.182	38	26				70	Shale
24-3	715			2.078	37	24				71	Shale
25-2	723			2.100	37	25				59	Shale
26-3	734			2.207	30	17				75	Shale
27-3	753			2.003	42	27				92	Claystone
28-3	771			2.032	40	25		3.129			Claystone
28-3	772			2.559	8	4				120	Claystone
30-3	810			2.122	36	21	1.715			108	Argillaceous limestone
31-3	828			2.132	34	18				180	Claystone
32-3	838			1.996	33	21	1.822	2.108		105	Argillaceous siltstone
34-1	873			2.562	11	4	3.245	3.529		131	Calcareous siltstone
34-3	876			2.194	31	17		1.830			Calcareous shale
35-2	884			2.268	25	15		2.240		115	Marlstone
38-3	942			2.281	28	14	2.008	2.278		105	Silty marlstone
39-4	953			2.282	31	19				105	Silty marlstone
41-2	988			2.377	23	12		2.451		88	Silty marlstone
41-2	988			2.251	27	17	2.219	2.219			Silty marlstone
42-3	1010			2.317	28	16	1.984	2.134		75	Silty marlstone
43-2	1026			2.679	5	3	1.635	3.617		115	Calcareous siltstone
44-3	1047			2.338	18	11	2.136	2.262		35	Silty claystone
45-3	1067			2.378	21	13	1.997	2.023		60	Silty claystone
47-3	1105			2.682	3	2	4.367	4.222		137	Calcareous siltstone
51-2	1168						4.203	3.824			Calcareous siltstone

siliceous limestones produced velocities on the order of 2.5 to 2.8 km/sec.

A stable increase in porosity values up to 45% and associated decrease in velocities is found below a depth of 600 meters. Porosity values tend to decrease thereafter, approaching 20% at 800 meters, where velocity data have a range of between 2.5 and 2.8 km/sec. A calcarenite sample from 740 meters produced a porosity of 41% and velocity of 1.95 (vertical) and 2.12 (horizontal) km/sec. The low velocities and related increase in porosity below 680 meters are associated with lower Eocene argillaceous limestones and marls which are devoid of siliceous material.

Site 367

Site 367 was located in the Cape Verde Basin. The site was abandoned upon coring basalt below upper Jurassic (Kimmeridgian, or older) argillaceous limestone.

Four major lithologic units may be defined, according to their physical property characteristics. A silty-clay zone containing some zeolites extends down to the

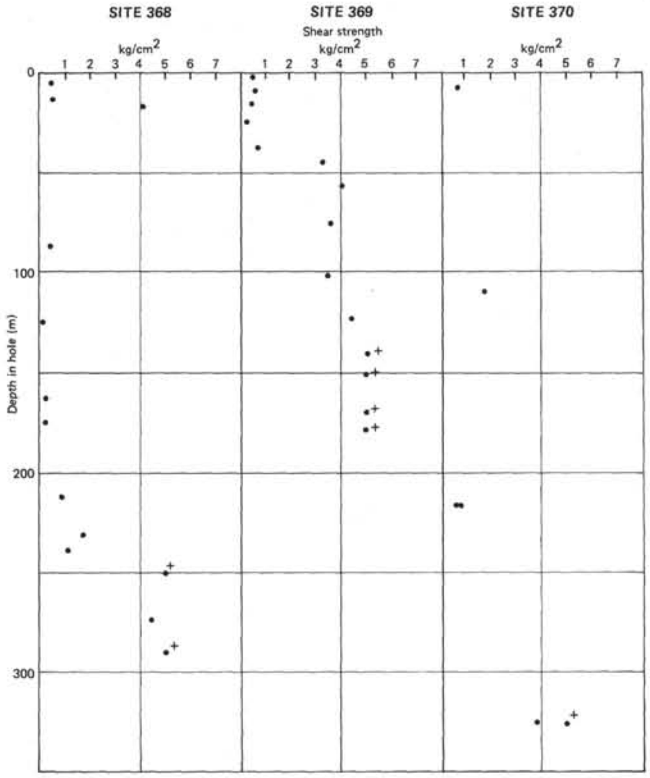

Figure 2. *Shear strength profiles for Sites 368, 369, and 370.*

upper Cretaceous at about 620 meters below the sea floor. Below this sequence a gassy black claystone/shale unit, dated as Cenomanian-Albian in age, extends to approximately 840 meters. Between the latter zone and the basalt, cored at 1144 meters, the sediments consisted of a variety of well-cemented limestones.

The pososity data, plotted in Figure 4, have an overall decrease with depth from 65% to less than 10% within the lower limestone unit. The values are highly scattered reflecting the large variation in lithology encountered at this site. Limestones below 840 meters have porosities of less than 30% and are segregated in Figure 4 by a dashed line. The wide variability of porosities in the uppermost 500 meters reflects a variety of sediments which include marls, clays, zeolitic clays, and varying admixtures of sand. The various combinations of grain size are believed responsible for the wide range of porosities (39% to 74%).

Velocity data are lacking throughout the clay, sand, and shale sequence due to the brittle and expanding nature of these sediments when retrieved aboard *Glomar Challenger*. Velocities within the uppermost marls ranged from 1.49 km/sec to 1.66 km/sec. These values, however, were obtained on disturbed samples and consequently reflect a lower velocity limit. Velocities obtained within the various limestone units display a high degree of anisotropy as well as a wide range of velocities. The latter run from 2.0 km/sec up to 4.4 km/sec with purer limestones having higher velocities than those which are argillaceous.

A mini core obtained within a homogeneous fine-grained section of basalt drilled at 1150 meters produced a velocity of 4.26 km/sec.

Summary

Four major lithofacies may thus be recognized at Site 367 according to their physical properties.

1) A silty-clay unit above 625 meters composed of nanno-foram marls and clays, diatomaceous clays, zeolite clays with a few cherts (porosity value of 39% at 373 meters) and a multicolored variegated silty clay. This sequence reflects a transition from unconsolidated to well indurated silty clays with velocities below 2.0 km/sec.

2) The second unit consists of a gassy shale/mudstone which includes a few intercalated limestones. Velocities on retrieved samples were too attenuated to be measured due to the large gaseous phase.

The intercalated limestones in the sequence increase in relative percentage towards the base, where the unit becomes entirely limestone. Porosity within the shales is somewhat meaningless due to the presence of gas. The specific gravity values strongly reflect the large amount of organic matter, with values as low as 1.65 g/cc.

3) This unit consists of a large variety of limestone which exhibit variations in the physical properties according to their carbonate and clay content.

4) The basalts recovered at the base of the hole were only measured for velocity and specific gravity. Calcite veins were present, although their effects on the acoustic velocities were not determined.

Site 368

Three major lithofacies were encountered at Site 368: (1) foram-nanno oozes and marls ranging from Pleistocene to lower Miocene in age; (2) unit 1 progressively grades into a silty clay sequence (Unit 2) at 266 meters; this second unit consists of multicolored (mostly green) silty clays grading into siltstones with interbedded chert (below 350 m) and a few volcanic ash layers between 230 and 250 m; (3) black shales below 950 meters in which a limestone bed, two thin (10 cm) and a thicker (12.5 m) diabase layers were found interbedded.

Porosities decrease from 74% to 52% within the nanno oozes and marls while exhibiting a large degree of variability below a depth of 150 meters, as illustrated in Figure 5. Between 150 and 400 meters the mass physical properties data are erratic due to the cyclic and lithologic variations found at the base of Unit 1 and top of Unit 2. This zone grades from loose nanno oozes to silty claystones with numerous interbeds which include: marls, clays, silty clays, and several volcanic ash layers. Velocity data throughout this zone reflect similar variability and resulted in poor velocity data within this portion of the hole.

Below a depth of 400 meters physical properties data exhibit a slight increase in porosity data from 60% to a maximum of 68% at 516 meters (Figure 5) within the cyclic green claystones of Lithologic Unit 2. Due to the friable nature of these claystones, velocity measure-

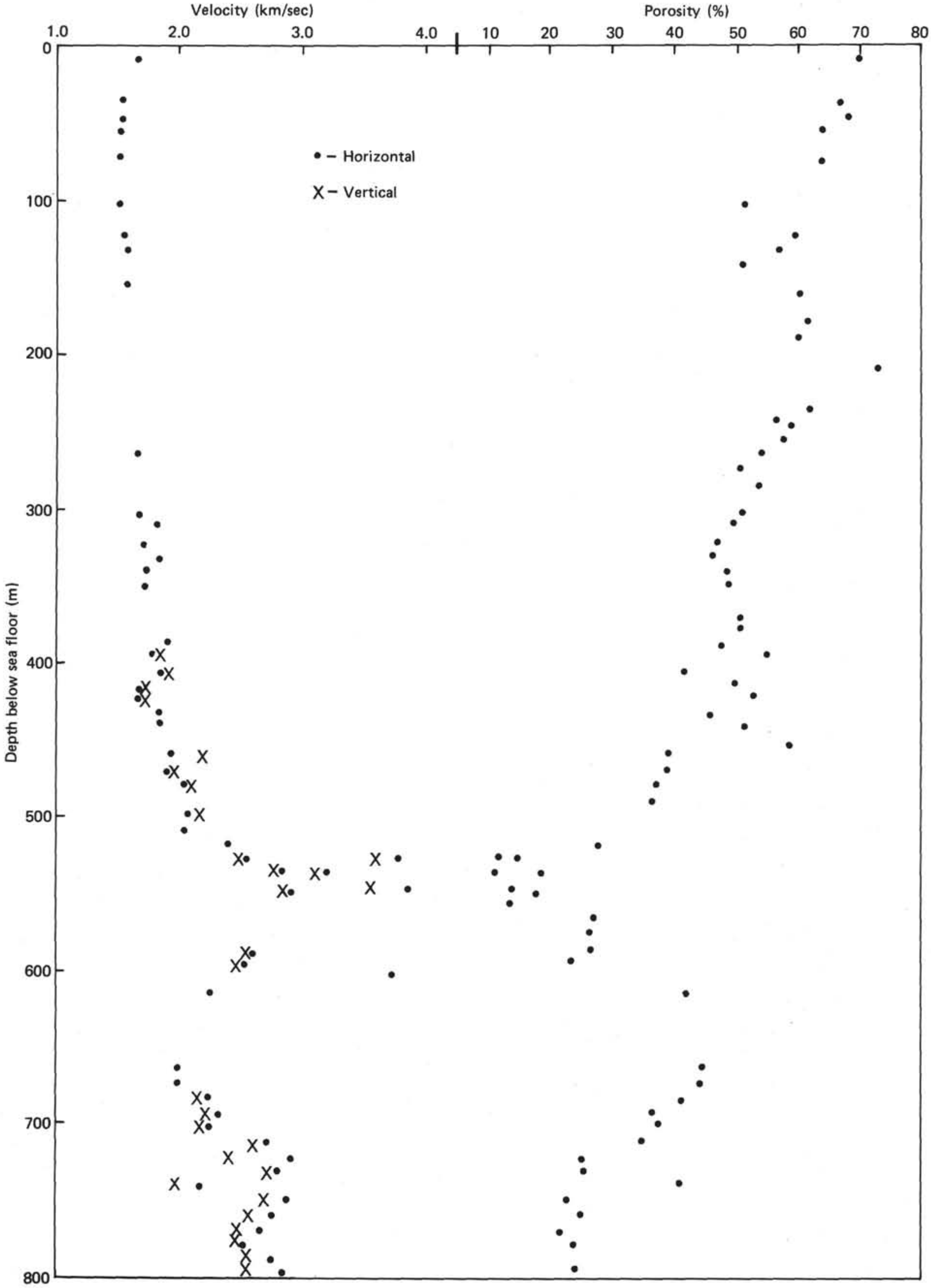

Figure 3. *Plot of porosity and velocity data versus depth, Site 366.*

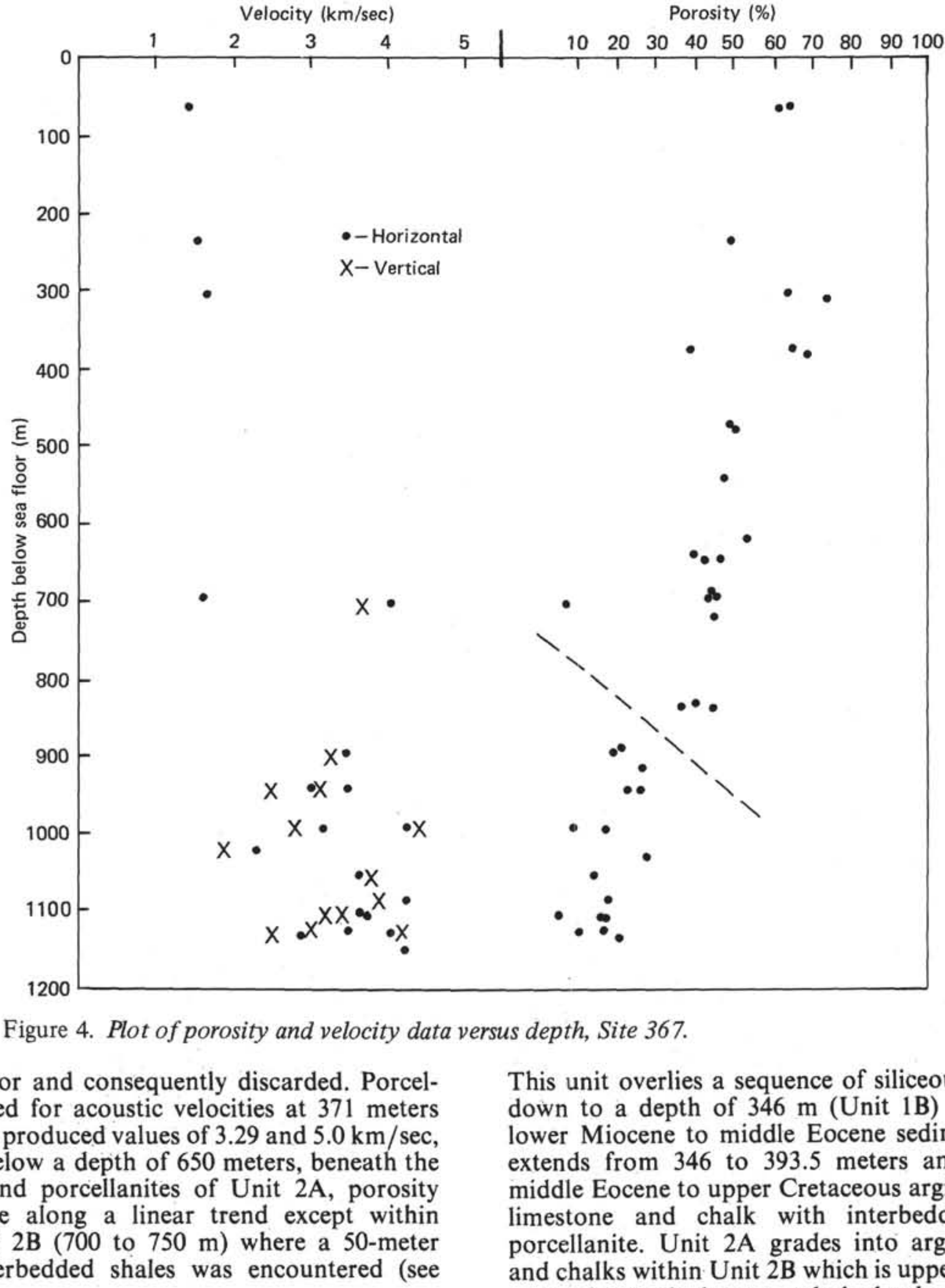

Figure 4. *Plot of porosity and velocity data versus depth, Site 367.*

ments were poor and consequently discarded. Porcellanites measured for acoustic velocities at 371 meters and 585 meters produced values of 3.29 and 5.0 km/sec, respectively. Below a depth of 650 meters, beneath the lower cherts and porcellanites of Unit 2A, porosity values decrease along a linear trend except within lithologic Unit 2B (700 to 750 m) where a 50-meter section of interbedded shales was encountered (see Figure 5).

Black organic-rich shales encountered about the diabase sills of Lithologic Unit 3 displayed large variability in porosity which ranged between 53% and 32%. The diabase sill encountered at 951 meters produced a velocity of 3.55 km/sec. A rough linear trend of decrease in porosity has been sketched in Figure 5.

Site 369

Site 369 was drilled midway down the continental slope into the continental side of an anticlinal feature. Five major lithologic units were encountered, which include a series of nanno marls down to 127.5 m (Unit 1A), ranging in age from Quaternary to lower Miocene. This unit overlies a sequence of siliceous nanno marls down to a depth of 346 m (Unit 1B) which includes lower Miocene to middle Eocene sediments. Unit 2A extends from 346 to 393.5 meters and consisted of middle Eocene to upper Cretaceous argillaceous nanno limestone and chalk with interbedded chert and porcellanite. Unit 2A grades into argillaceous marls and chalks within Unit 2B which is upper Cretaceous in age and extends down to a hole depth of 422 m. Below Unit 2 occur silty nanno marls, which are upper Albian, to the final hole depth of 488.5 m. Measured bulk properties data and acoustic velocities are presented in Table 1 with a plot of porosity and velocity versus depth illustrated in Figure 6. No GRAPE values were obtained due to rotation of the core barrel during drilling operations, which produced spiral grooves in the core samples.

The results of shipboard porosity measurements indicate a slight scatter along a linear decrease in values down to the upper Albian sediments. Values range from 68% to 6% while the general trend is a net reduction from about 60% at the sea floor to 40% at the greatest depth drilled. Very low porosity values were

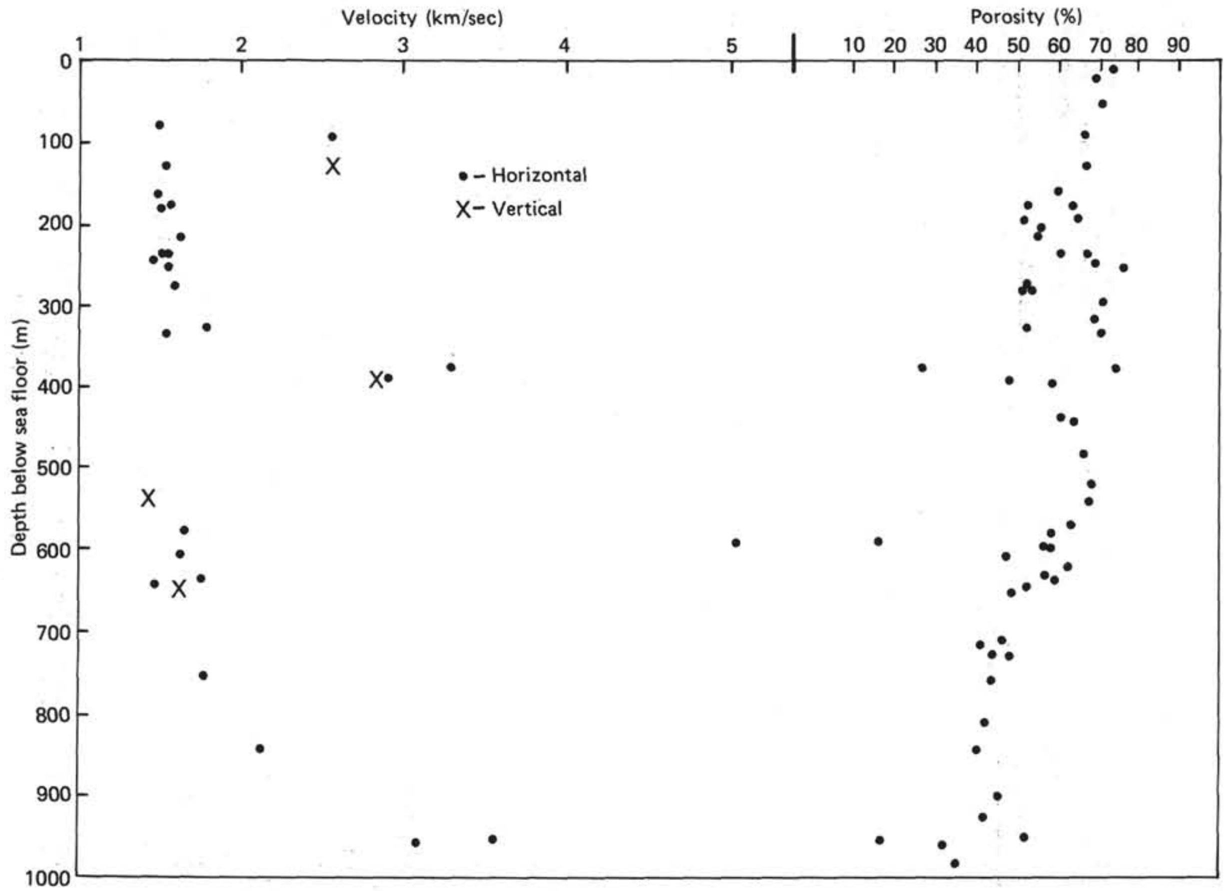

Figure 5. *Plot of porosity and velocity data versus depth, Site 368.*

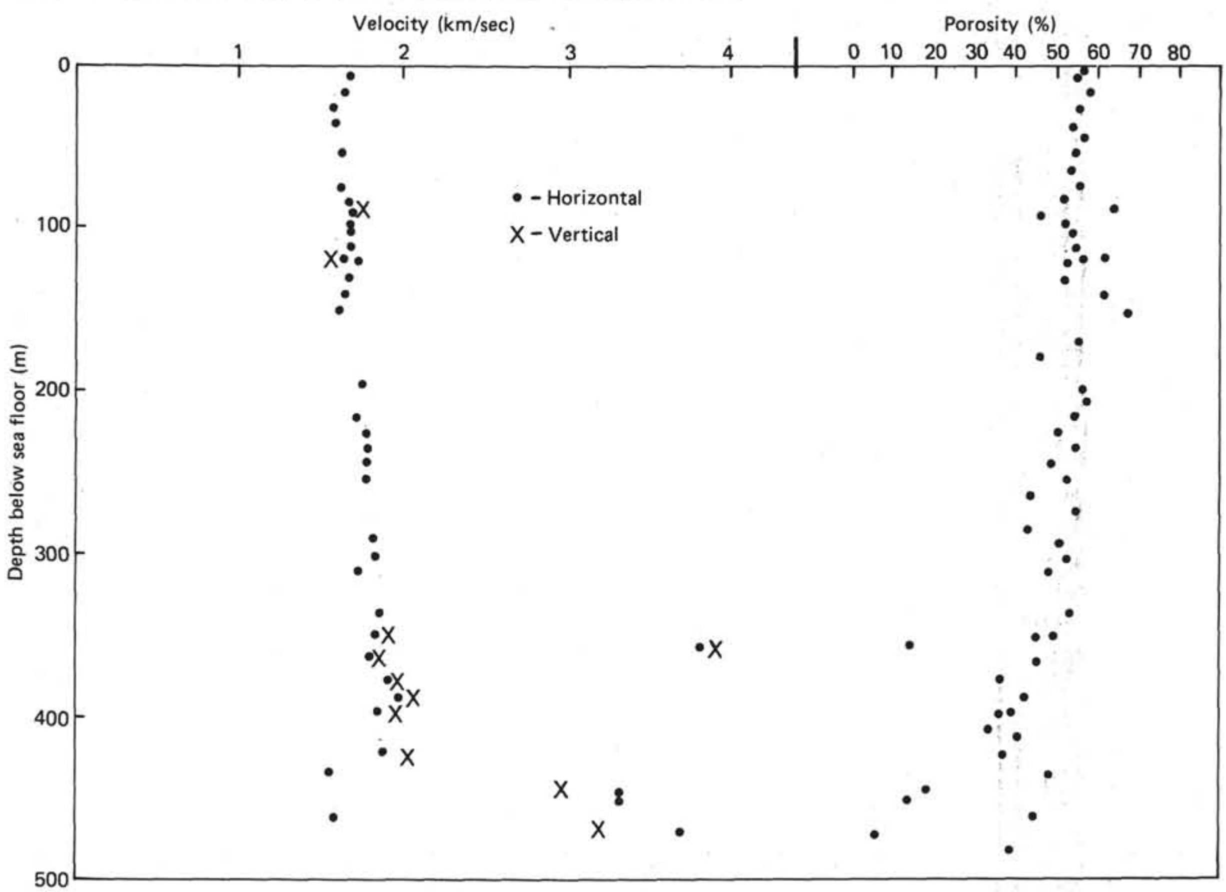

Figure 6. *Plot of porosity and velocity data versus depth, Site 369.*

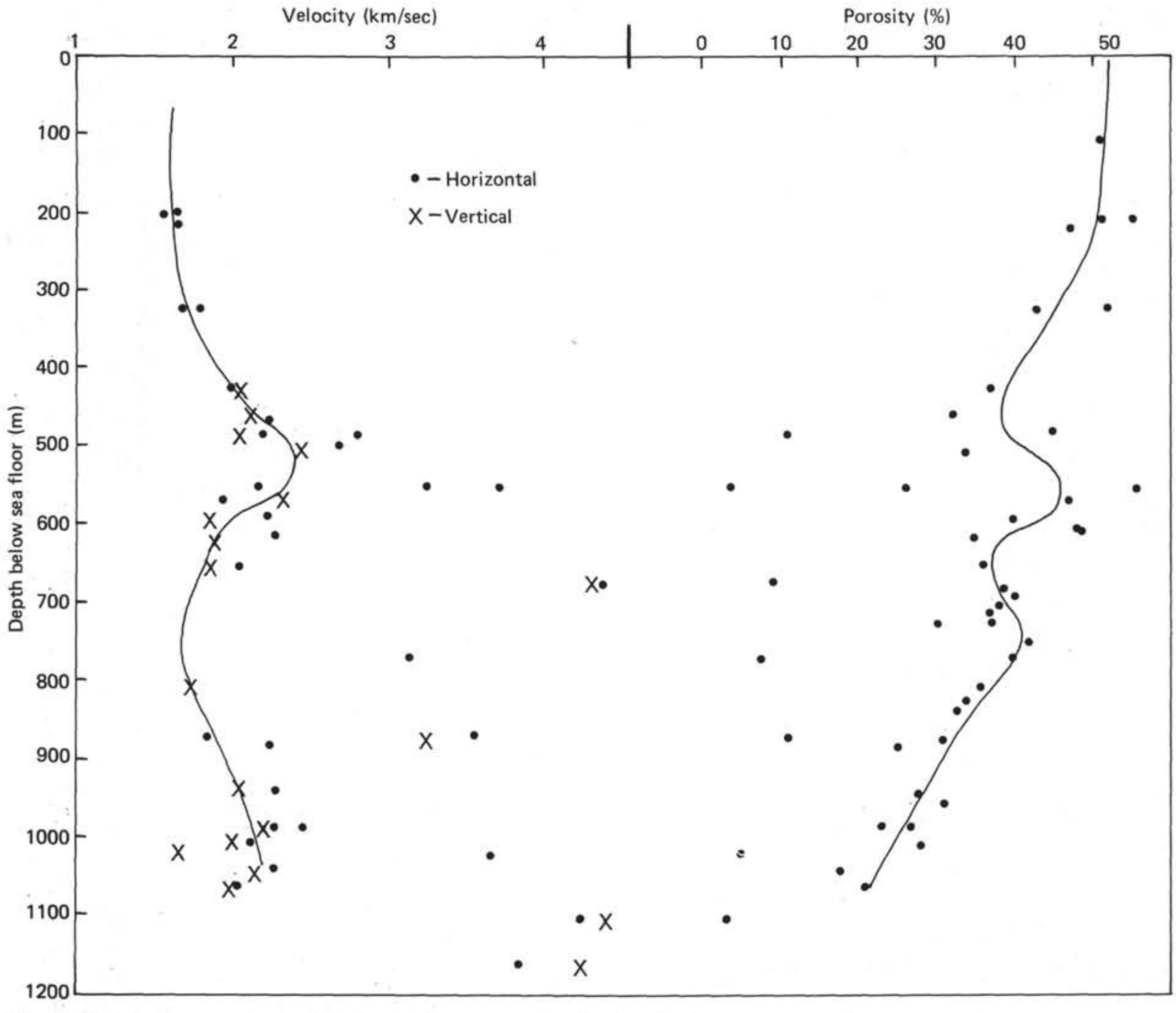

Figure 7. *Plot of porosity and velocity data versus depth, Site 370.*

obtained within porcellanite retrieved at 358 meters, marlstone and chalk from 450 meters, and within a gypsum and marlstone sample from a depth of 473 meters.

Velocity measurements on cored samples indicate a linear increase from 1.55 km/sec at sea floor to just over 2.0 km/sec at a depth of 425 meters. Unusually high velocities were obtained within the aforementioned low porosity samples as depicted in Figure 6. The porcellanite at 358 meters may thus be considered atypical in view of the bed thickness of a few centimeters. Several velocity measurements were obtained within the slump feature centered about a depth of 300 meters; these ranged between 1.75 and 1.88 km/sec and represent a narrow spread for the sedimentological variety within this feature.

Site 370

A plot of porosity and velocity values with depth for Site 370 is presented in Figure 7. These data show several irregularities associated with the various lithologies encountered. The uppermost sedimentary Units 1 through 3A display a decrease in porosity from over 50% (in Quaternary clays) at the seafloor to less than 40% within a calcareous silty clay of upper Eocene age. Shipboard measured velocities within this interval exhibit a related increase from 1.55 km/sec to over 2.4 km/sec. At a depth of approximately 460 meters a net decrease in porosity and associated increase in velocity is observed in the calcareous silty clays (and porcellanites) of Lithologic Unit 3B. This feature is believed to be associated with the observed increase in cementation of the clay sediments and the occurrence of porcellanite. Porosity values decrease once more within Lithologic Unit 3C at a depth of 530 meters in a thick sequence of turbidites composed of calcareous silty clay with silt, sand, porcellanite, and chert. Acoustic velocities tend to decrease, while values ranging between 3.0 km/sec and 4.5 km/sec occur in the cherts and porcellanites which similarly display porosities of less than 20%.

Lithologic Unit 4 contains relatively higher porosities (above 40%) measured within a thin sequence of nanno marls which gradually grade into nanno-bearing claystone of Unit 5A. Below a depth of 750 meters the effect of cementation reduces porosities linearly from 40% to 20% at the maximum depth drilled of 1176.5 meters.

Velocity and porosity values are scattered about two semiparallel lines with depth at the lower half of Site 370 as a result of the frequent occurrence of cherts, porcellanites, and cemented sandstones.

CONSOLIDATION TESTS SITE 368

Consolidation characteristics provide an additional tool for the understanding of depositional processes and the history of sediment accumulation within ocean basins. Also, the data provide engineering criteria for the sediment-bearing capacity, and slope-stability problems. However, little work has been published on mass physical properties and even less on consolidation characteristics. Samples from DSDP Leg 10, Leg 16 (Keller and Bennett, 1973), Leg 18 (Lee, 1973), and Leg 31 (Trabant et al., 1975) had been evaluated for their consolidation characteristics and associated geotechnical properties prior to the work described here.

Consolidation refers to the reduction in volume of a sediment under an imposed load, while the synonymous term "compaction" is employed with reference to the process of hardening or lithification of a sediment. Four samples obtained at Site 368, composed predominantly of terrigenous sediments, were consolidated in the laboratory according to standard procedures (Lambe, 1951). The consolidometer apparatuses were back-pressure units (Lowe et al., 1964) in which a back pressure of 7 atm was maintained on the samples throughout the duration of the tests. This permits the near-total redissolution of any gases due to the removal of hydrostatic pressure, associated with sample retrieval.

The consolidation test, in the very simplest of terms, consists of the application of a normal (vertical) load (pressure) upon a small (4.45 cm or 6.125 cm diameter) free-draining, confined, cylindrical sample of sediment. The loads are increased with time and are usually doubled at 24-hour intervals, while the rate and amount of volume decrease under each load are recorded. The results of the tests are displayed in Figures 8 through 11 as a plot of void ratio (volume of voids divided by the volume of solids) versus the log of normal pressure, commonly referred to as an e-log p curve. This curve serves as the basis for settlement calculations, as well as determining the proconsolidation pressure (the greatest load to which a sediment has been subjected).

Consolidation tests normally provide a means whereby the depositional history of an accumulation of sediments can be determined. In soil mechanics terminology, a deposit is said to be normally consolidated if the effective overburden pressure (*Po*) is equal to the preconsolidation pressure (*Pc*). The effective overburden pressure acting on an in situ sample is equal to the difference between the overburden pressure (*Po*) or stress and the pore water pressure. The total overburden stress is the combined wet-bulk density of the overlying sediments minus the unit weight of the water. Thus, to determine the effective pressure, acting on a sample in place, one needs to know the difference between the expected hydrostatic and in situ pore-water pressure. In spite of the lack of in situ pore-pressure measurements, a good first-order approximation of the in-place effective overburden pressures is obtained as the total stress from the reported wet-bulk-density measurements.

If the computed overburden pressure is greater than the preconsolidation pressure, the sediment is said to be underconsolidated, that is, the sediment does not appear to have consolidated (drained its excess pore

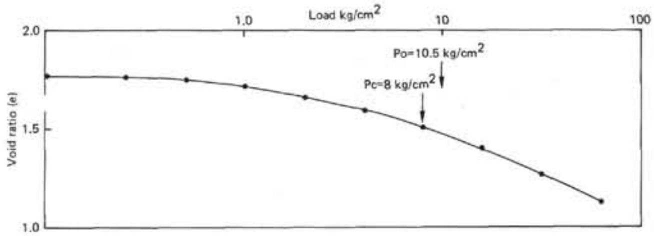

Figure 8. *Consolidation test, Site 368, 175 meter depth, e-log P curve.*

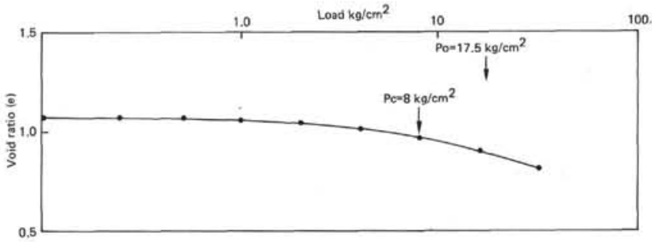

Figure 9. *Consolidation test, Site 368, 275 meter depth, e-log P curve.*

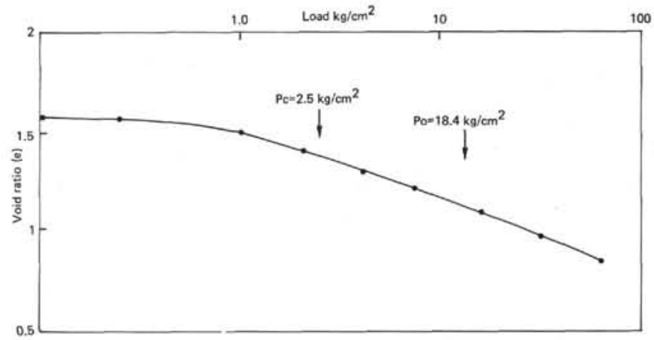

Figure 10. *Consolidation test, Site 368, 288 meter depth, e-log P curve.*

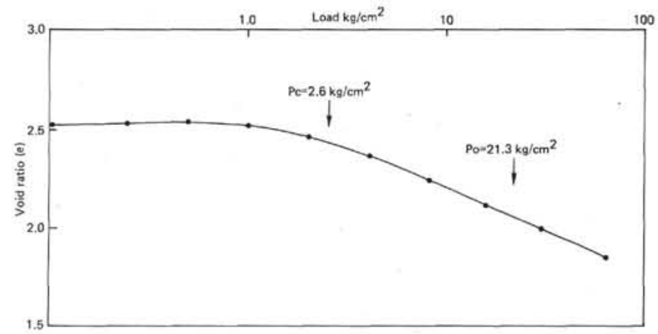

Figure 11. *Consolidation test, Site 368, 330 meter depth, e-log P curve.*

pressure) under its present load. On the other hand, if the overburden pressure is less than the preconsolidated pressure, the sediments are said to be overconsolidated. Underconsolidated sediments commonly occur in areas of rapid sedimentation such as deltas (Fisk and McClelland, 1959) and are due to insufficient time for the drainage of pore water (Moore, 1964). Sample disturbance may also produce underconsolidation. Conversely, overconsolidated sediments may be the result of the removal of overlying sediment (reduction in overburden), desiccation of sediments, unusual physicochemical interparticle binding or cementation, or any externally applied stress.

The four consolidation tests were performed upon Miocene pelagic clays obtained within Lithologic Unit 2B, each of which is described below with respect to sample depth at Site 368.

175 meters—Besides a fine fraction of clays, this sample contained coarse material including pyrite, pteropods, and a few well-preserved fish teeth. The e-log P curve of Figure 8 indicates a gradual "break" which provided an approximate preconsolidation pressure (*Pc*) of 8 kg/cm² according to the Casagrande method (1936). In comparision to the computed overburden stress (*Po*) of 10.5 kg/cm² (employing an average bulk density of 1.60 g/cc) the difference in stress is not particularly significant.

275 meters—The coarse fraction of this silty clay sample contained pyrite, fish teeth, calcite pellets, and shallow water benthic forams. The slight "break" in the e-log P curve rendered the determination of *Pc* difficult. A preconsolidation value of 8 kg/cm² indicates a net underconsolidation of 9.5 kg/cm² when compared to the average bulk density calculated overburden for this depth of 17.5 kg/cm².

288 meters—The Miocene silty clay sample from this depth contained a few calcareous benthic foraminifera and some aeolian quartz grains. The measured initial void ratio of 1.56 is high for such sediments at this depth and is evident in the calculation of the preconsolidational pressure of 2.5 kg/cm². An overburden stress based upon an average bulk density of 1.70 g/cc produced a value of 18.4 kg/cm². The difference between these two values amounts to 15.9 kg/cm² indicating a high degree of underconsolidation.

330 meters—The sample consolidate from this depth contained a coarse grain fraction composed of pyrite and quartz grain filling within burrow tubes. The tested sample had an initial void ratio of 2.53, a very high value for this depth. The e-log P curve of Figure 11 exhibits a break in slope which produced a preconsolidation figure of 2.6 kg/cm². The computed overburden stress (*Po*), by use of an average cumulative bulk density of 1.7 g/cc, gave a value of 21.3 kg/cm², nearly tenfold that of the laboratory determined maximum past stress. A value of 18.7 kg/cm² may thus be attributable to underconsolidation, possible excess pore pressures, or sample disturbance.

Summarizing these consolidation test data, one finds an ever increasing degree of underconsolidation with depth.

The values are 2.5, 9.5, 15.9, and 18.7 kg/cm² at the respective sample depths of 175, 275, 288, and 330 meters at Site 368. The samples were specifically selected to follow a trend of increased porosity values (depicted in Figure 5) below a subbottom depth of 200 meters.

Although the underconsolidated nature of the tested samples may be attributed to coring disturbance, this would appear unlikely in view of sample selection, the trend towards an increase in underconsolidation values with depth, and the results of similar investigations on DSDP samples (e.g. Keller and Bennett, 1973). More samples from Leg 41, tested for their consolidation characteristics, may provide valuable data towards the above trend as well as confirm the precise nature of the sudden increase in shear strengths at a depth of 40 meters at Site 369.

VELOCITY COMPARISONS, ALL SITES

As stated earlier, velocity (P-wave) measurements were made in both the horizontal and vertical directions on samples collected during Leg 41. While specific values are listed in Table 1, Figure 12 is a plot of measurements made in both directions to illustrate the anisotropic velocity effects within the sediments. The dashed line of Figure 12 represents no anisotropy and reveals the trend towards greater measured velocities in the horizontal plane. As discussed by Marshall (1975) this directional dependence is attributed to the presence of unsilicified or less silicified (porcellanite) interlayers within cherts. Similarly within lesser cemented calcareous and terrigenous samples, velocity measurements reflect the higher interlayer values when measured horizontally. Vertical velocity measurements, on the other hand, reflect average interlayer velocities within the nonhomogeneous minutely layered cemented sediment samples. It thus appears that the anisotropy of measured acoustic velocities is attributable to sedimentological variations within sampled sediments.

Figure 13 represents a plot of the measured acoustic velocities (P-wave) versus porosity for Sites 366 through 370 of Leg 41. No attempt was made to classify the data according to lithologic type, however, the greater velocities (above 2.0 km/sec) are indicative of well cemented limestones and cherts. The dashed line represents the solution of the empirical equation derived by Nafe and Drake (1957) for $n = 5$ (an empirical value) and is presented for reference only. The data collected during Leg 41 display a relatively large scatter, which is possibly due to the correspondingly wide variety of sediments encountered. Lithologies represented in Figure 13 include oozes, clays, claystones, chalks, limestones, cherts, and basalt. The plot is nonetheless typical for marine sediments as discussed by Nafe and Drake (1963).

A plot of drilling rate versus acoustic velocity (horizontally measured P-waves) shown in Figure 14 is too highly scattered to draw a meaningful relationship. Correlating shear strengths to drilling rate also provided no apparent relationship. It thus appears that factors other than lithology and sediment physical properties are responsible for major variations in drilling rates. A very general trend with a low correlation coefficient is nevertheless discerned in the plot of Figure 14.

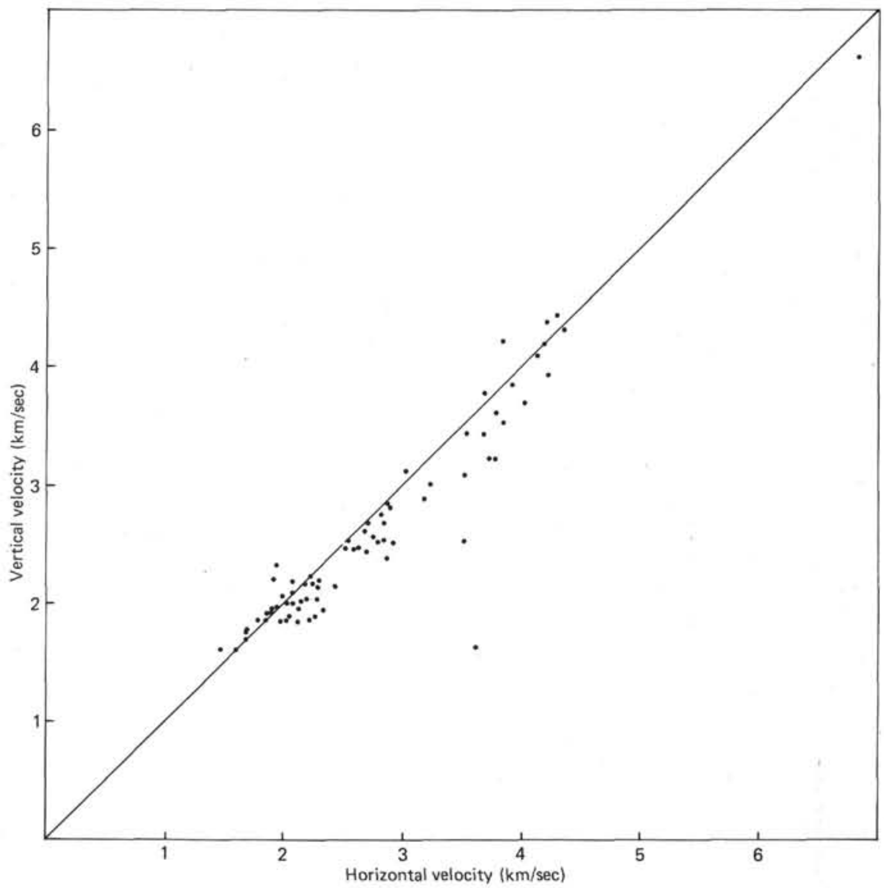

Figure 12. *Plot of horizontal versus vertical measured P-wave velocities for all Leg 41 sites.*

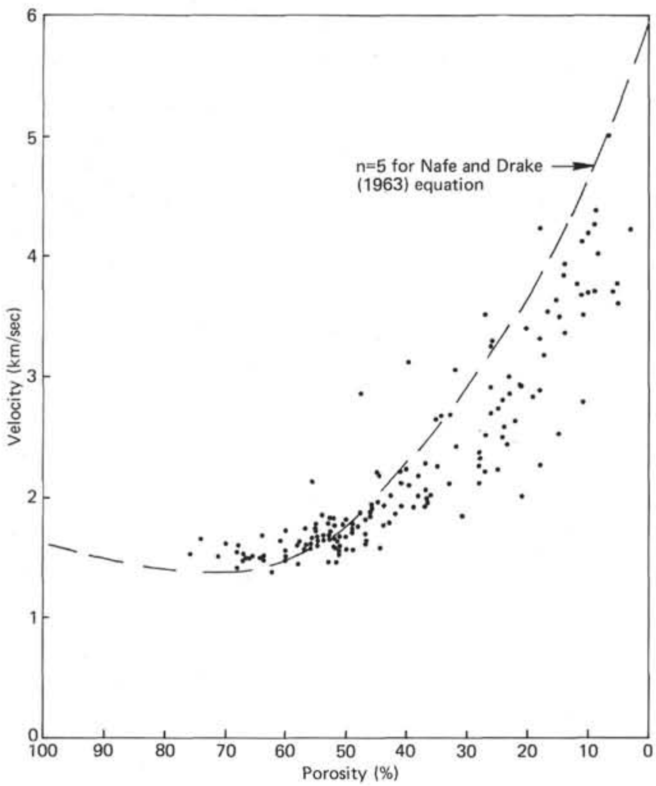

Figure 13. *Porosity plotted against velocity for all Leg 41 sites.*

REFERENCES

Bennett, R.H. and Keller, G.H., 1973. Physical properties evaluation. *In* van Andel, Tj.H., Heath, G.R., et al., Initial Reports of the Deep Sea Drilling Project, Volume 16: Washington (U.S. Government Printing Office), p. 513-519.

Boyce, R.E., 1973a. Instructions for Hamilton-Frame Velocimeter, Deep Sea Drilling Project: Scripps Institute of Oceanography, La Jolla, California, p. 19.

_______, 1973b. Instructions for shear strength measurement of clays by vane shear techniques: Deep Sea Drilling Project, Scripps Institute of Oceanography, La Jolla, California, p. 47.

_______, 1975. Definitions and laboratory techniques of compressional sound velocity parameters and wet water content, wet-bulk density, and porosity parameters by gravimetric and gamma ray attenuation techniques. *In* Schlanger, S.O., Jackson, E.D., et al., Initial Reports of the Deep Sea Drilling Project, Volume 33: Washington (u.S. Government Printing Office), p. 931-951.

Casagrande, A., 1936. The determination of the preconsolidation load and its practical significance. Proc. First Intern, Conf. Soil Mech. Foundation Engineering. 60.

Fisk, H.N. and McClelland, B., 1959. Geology of continental shelf off Louisiana: its influence on offshore foundation design: Geol. Soc. Am. Bull., v. 70, p. 1369.

Hottman, W.E., in press. In Bolli, H., Ryan, W.F.B., et al. Initial Reports of the Deep Sea Drilling Project, Volume 40, Washington (U.S. Government Printing Office).

Keller, G.H. and Bennett, R.H., 1973. Sediment mass physical properties—Panama Basin and Northeastern Equatorial Pacific. *In* van Andel, Tj. H., Heath, G.R., et

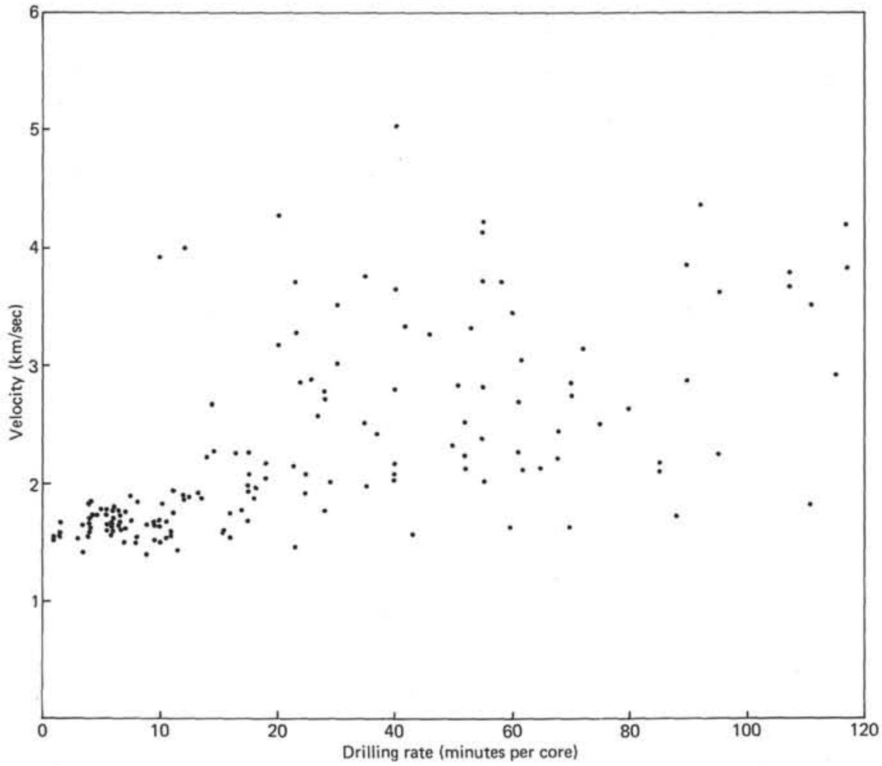

Figure 14. *Plot of velocities (all sites) versus drilling rate.*

al., Initial Reports of the Deep Sea Drilling Project, Volume 16: Washington (U.S. Government Printing Office), p. 499-512.

Lambe, T.W., 1951. Soil testing for engineers: New York (John Wiley and Sons).

Lee, H.J., 1973. Measurements and estimates of engineering and other physical properties, Leg 19. *In* Creager, J.S., Scholl, D.W. et al., Initial Reports of the Deep Sea Drilling Project, Volume 19: Washington (U.S. Government Printing Office), p. 701-720.

Lowe, J., III, Zaccheo, P.F., and Feldman, H.S., 1964. Consolidation testing with back pressure: J. Soil Mech. Found., Div. Am. Soc. Civil Engrs., v. 90, p. 69.

Marshal, M.C., 1975. Unpublished site reports for Leg 32 of the Deep Sea Drilling Project.

Moore, D.G., 1964. Shear strength and related properties of sediments from experimental Mohole (Guadalupe site): J. Geophys. Res., v. 69, p. 4271.

Nafe, J.E., and Drake, C.L., 1957. Variation with depth in shallow and deep water marine sediments of porosity, density and the velocities of compressional and shear waves: Geophysics, v. 22, p. 523-552.

———, 1963. Physical properties of marine sediments, *In* Hill, M.N. (Ed.), The sea, v. 3, New York (John Wiley and Sons).

Rocker, K., 1974a. Physical properties measurements and test procedures of Leg 27. *In* Veevers, J.J., Heirtzler, J.R., et al., Initial Report of the Deep Sea Drilling Project, Volume 27: Washington (U.S. Government Printing Office), p. 433-443.

———, K., 1974b. Vane shear strength measurements on Leg 27 sediment, *In* Veevers, J.J., Heirtzler, J.R., et al., Initial Reports of the Deep Sea Drilling Project, Volume 27: Washington (U.S. Government Printing Office), p. 425-432.

Trabant, P.K., Bryant, W.R., and Bouma, A.H., 1975. Consolidation characteristics of sediments from Leg 31 of the Deep Sea Drilling Project. *In* Karig, D.E., Ingle, J.C., Jr., et al. Initial Reports of the Deep Sea Drilling Project, Volume 31: Washington (U.S. Government Printing Office).